Swiss J Geosci (2012) 105:463–476
DOI 10.1007/s00015-012-0116-2

Earthquakes in Switzerland and surrounding regions during 2011

Nicholas Deichmann · John Clinton · Stephan Husen · Benjamin Edwards · Florian Haslinger · Donat Fäh · Domenico Giardini · Philipp Kästli · Urs Kradolfer · Stefan Wiemer

Received: 15 September 2012 / Accepted: 19 October 2012 / Published online: 25 November 2012

Abstract This report of the Swiss Seismological Service summarizes the seismic activity in Switzerland and surrounding regions during 2011. During this period, 522 earthquakes and 92 quarry blasts were detected and located in the region under consideration. With a total of only 10 events with $M_L \geq 2.5$, the seismic activity in the year 2011 was far below the average over the previous 36 years. Most noteworthy were the earthquake sequence of Sierre (VS) in January, with two events of M_L 3.3 and 3.2, the M_L 3.3 earthquake at a depth of 31 km below Bregenz, and the M_L 3.1 event near Delémont. The two strongest events near Sierre produced shaking of intensity IV.

Keywords Seismicity · Focal mechanisms · Magnitude >3 · Sierre · Bregenz · Delémont

Zusammenfassung Dieser Bericht des Schweizerischen Erdbebendienstes stellt eine Zusammenfassung der im Vorjahr in der Schweiz und Umgebung aufgetretenen Erdbeben dar. Im Jahr 2011 wurden im erwähnten Gebiet 522 Erdbeben sowie 92 Sprengungen erfasst und lokalisiert. Mit nur 10 Beben der Magnitude $M_L \geq 2.5$, lag die seismische Aktivität im Jahr 2011 weit unter dem Durchschnitt der vorhergehenden 36 Jahre. Die bedeutendsten Ereignisse waren die Erdbebensequenz von Sierre im Januar mit zwei Beben der Magnitude M_L 3.3 und 3.2, das Beben in 31 km Tiefe bei Bregenz (M_L 3.3) sowie das Beben bei Delémont (M_L 3.1). Die zwei stärksten Beben von Sierre haben Erschütterungen der Intensität IV verursacht.

Resumé Le présent rapport du Service Sismologique Suisse résume l'activité sismique en Suisse et dans les régions limitrophes au cours de l'année 2011. Durant cette période, 522 tremblements de terre et 92 tirs de carrière ont été détectés et localisés dans la région considérée. Avec seulement 10 événements de magnitude $M_L \geq 2.5$, l'activité sismique de l'année 2011 est en dessous de la moyenne des 36 années précédentes. Les événements les plus significatifs étaient la séquence de Sierre au début de janvier, avec deux tremblements de magnitude M_L 3.3 et 3.2, le tremblement à une profondeur de 31 km près de Bregenz (M_L 3.3) ainsi que un tremblement près de Delémont (M_L 3.1). Les deux événements de Sierre ont provoqué des secousses d'intensité IV.

1 Introduction

Past earthquake activity in and around Switzerland has been documented in an uninterrupted series of annual reports from 1879 until 1963 (*Jahresberichte des Schweizerischen Erdbebendienstes*). Three additional annual reports were published for the years 1972–1974. These reports together with historical records of earthquakes dating back to the 13th century have been summarized by Pavoni (1977) and provided the basis for the first seismic hazard map of Switzerland (Sägesser and Mayer-Rosa 1978). With the advent of routine data processing by computer, the wealth of data acquired by the nationwide

N. Deichmann (✉) · J. Clinton · S. Husen · B. Edwards · F. Haslinger · D. Fäh · D. Giardini · P. Kästli · U. Kradolfer · S. Wiemer
Swiss Seismological Service, ETH Zürich, Sonneggstrasse 5, 8092 Zürich, Switzerland
e-mail: deichmann@sed.ethz.ch
URL: http://www.seismo.ethz.ch

seismograph network were regularly documented in bulletins, with detailed lists of all recorded events (*Monthly Bulletin of the Swiss Seismological Service*). Since 1996, annual reports summarizing the seismic activity in Switzerland and surrounding regions have been published in the present form (Baer et al. 1997, 1999, 2001, 2003, 2005, 2007; Deichmann et al. 1998, 2000a, 2002, 2004, 2006, 2008, 2009, 2010, 2011). In the course of reassessing the seismic hazard in Switzerland, a uniform earthquake catalogue covering both the historical and instrumental periods was compiled in 2002 (Fäh et al. 2003). The official seismic hazard map of Switzerland based on this catalogue was released in 2004 (Giardini et al. 2004; Wiemer et al. 2009). In 2009, the Earthquake Catalogue of Switzerland was revised (ECOS-09) and is now available on-line (http://www.seismo.ethz.ch/prod/catalog/index). In addition, numerous studies covering different aspects of the recent seismicity of Switzerland have been published in the scientific literature (for an overview and additional references see, e.g. Deichmann 1990; Pavoni and Roth 1990; Rüttener 1995; Rüttener et al. 1996; Pavoni et al. 1997; Deichmann et al. 2000b; Kastrup et al. 2004; Kastrup et al. 2007). The present paper is the annual report on seismic activity in Switzerland for the year 2011.

2 Data acquisition and analysis

2.1 Seismic stations in operation during 2011

The Swiss seismological service (SED) operates two separate nationwide seismic networks: a high- gain, predominantly broad-band seismometer network (Table 1) and a low-gain accelerograph network (Table 2). The former is designed to continuously monitor the ongoing earthquake activity down to magnitudes well below the human perception threshold, whereas the latter is principally aimed at engineering concerns and thus focuses on recording so-called strong ground-motions in urban areas. In addition, the seismological service operates a number of temporary stations for various projects (Table 3).

The year 2011 saw some additions to the broad-band network (Fig. 1 and Table 1). Two new stations were added, at Grimsel Pass (GRIMS) and Pigniu (PANIX). The latter was constructed close to station LLS (Limmerensee) to ensure that the network continues to detect and produce high quality locations for earthquakes in the region, as construction on the Limmerensee dam, expected to continue until 2014, has significantly degraded the quality of recordings at LLS. Station GRIMS, which consists of both a broadband and a co-located strong-motion sensor, is located in a deep tunnel and fills a critical geographical gap in the seismic network. Thirteen stations in the network

Table 1 High-gain, three-component seismograph stations of the Swiss national network operational at the end of 2011 (Fig. 1)

National on-line network recorded in Zurich		
Code	Station name	Type
ACB	Acheberg, AG	EB
AIGLE	Aigle, VD	BB
BALST	Balsthal, SO	BB
BERNI	Bernina, GR	BB
BNALP	Bannalpsee, NW	BB, SM
BOURR	Bourrignon, JU	BB, SM
BRANT	Les Verrières, NE	BB
DAVOX	Davos, GR	BB
DIX	Grande Dixence, VS	BB, SM
EMBD	Embd, VS	BB
EMV	Vieux Emosson, VS	BB, SM
EWZT2	Wetzwil, ZH	SP
FIESA	Fiescheralp, VS	BB
FLACH	Flach, ZH	EB
FUORN	Ofenpass, GR	BB
FUSIO	Fusio, TI	BB, SM
GIMEL	Gimel, VD	BB
GRIMS	Grimsel, BE	BB, SM
GRYON	Gryon, VS	EB
HASLI	Hasliberg, BE	BB
LAUCH	Lauchernalp, VS	BB
LIENZ	Kamor, SG	BB, SM
LKBD	Leukerbad, VS	EB
LKBD2	Leukerbad, VS	SP
LLS	Linth-Limmern, GL	BB, SM
MMK	Mattmark, VS	BB, SM
MUGIO	Muggio, TI	BB
MUO	Muotathal, SZ	BB
PANIX	Pigniu, GR	BB
PLONS	Mels, SG	BB
SALAN	Lac de Salanfe, VS	EB
SENIN	Senin, VS	BB, SM
SIMPL	Simplonpass, VS	BB
SLE	Schleitheim, SH	BB
STEIN	Stein am Rhein, SH	EB
SULZ	Cheisacher, AG	BB, SM
TORNY	Torny, FR	BB
TRULL	Trullikon, ZH	EB
VANNI	Vissoie, VS	BB
VDL	Valle di Lei, GR	BB, SM
WEIN	Weingarten, TG	EB
WILA	Wil, SG	BB
WIMIS	Wimmis, BE	BB
ZUR	Ziirich-Degenried, ZH	BB, SM

Instrument type: *SP* 1 s, *EB* 5 s, *BB* broad-band, *SM* accelerometer
Signals of LKBD2 are transmitted via analogue telemetry

Table 2 Strong-motion stations of the Swiss national network with on-line data acquisition operational at the end of 2011 (Fig. 1)

On-line strong-motion network		
Code	Station name	Type
BIBA	Brigerbad, VS	SM
OTTER	Otterbach, BS	SM
SAUR	Augst-Römermuseum, AG	SM
SBAF	Basel-Friedhofgasse, BS	SM
SBAP	Basel-PUK, BS	SM
SBAT	Basel-Tropenhaus, BS	SM
SBIS2	Binningen, BS	SM
SBUA2	Buchs Kindergarten, SG	SM
SBUB	Buchserberg Malbun, SG	SM
SCEL	Celerina, GR	SM
SCHS	Schaffhausen Spital, SH	SM
SCOU	Cournillens, FR	SM
SCUC	Scuol-Clozza, GR	SM
SCUG	Chur Gewerbeschule, GR	SM
SEPFL	Lausanne EPFL, VD	SM
SFRA	Frenkendorf, BL	SM
SGEV	Genf Feuerwehr, GE	SM
SGRA	Grachen-Ausblick, VS	SM
SIOO	Sion-Ophtalmologie, VS	SM
SIOV	Sion-Valere, VS	SM
SKAF	Kaiseraugst-Friedhof, AG	SM
SLTM2	Linthal Matt, GL	SM
SLUB	Luzern Bramberg, LU	SM
SLUW	Luzern Werkhofstr., LU	SM
SMUK	Muraz-Kläranlage, VS	SM
SMUR	Muraz-Reservoir, VS	SM
SMZW	Muttenz-Waldhaus, BL	SM
SNIB	Sankt Niklaus, VS	SM
SOLB	Solothurn Schule Bruhl, SO	SM
SRER	Reinach Rainenweg, BL	SM
SRHB	Riehen-Bäumlihof, BS	SM
STAF	Tafers, FR	SM
STSP	Tschierv, GR	SM
SVIL	Visp-Litternaring, VS	SM
SVIO	Visp-ObereStapfeng., VS	SM
SVIT	Visp-Terbinerstr., VS	SM
SYVP	Yverdon Rue du Phil, VD	SM
SZER	Zernez, GR	SM

Instrument type (all three-component): *SP* 1 s, *SM* accelerometer

now include a strong motion sensor alongside the broadband sensor.

The ongoing densification of the strong-motion accelerograph network continued apace in 2011. Ten new stations were added (SBUA2, SCHS, SCUG, SEPFL, SGEV, SLUB, SLTM2, SOLB, SRER and SYVP, see Fig. 1 and Table 2).

Table 3 Local seismic networks with on-line data acquisition operational at the end of 2011

Code	Station name	Type
AlpTransit-Gotthard network		
CUNA	Cunera, GR	SP, SM
CURA	Curaglia, GR	SP
DOETR	Doetra, TI	SP, SM
LUKA1	Lucomagno, TI	SP, SM
NALPS	Val Nalps, GR	BB
RITOM	Lago Ritom, TI	SP, SM
TONGO	Tortengo, TI	SP
Noville network		
NOV1	St. Gingolph, VS	SP
NOV2	Port Valais, VS	SP
NOV3	Caux, VD	SP
NOV4	La tour de Pellz, VD	SP
Basel borehole network		
JOHAN	Sankt Johann (317)	SP
MATTE	Schiitzenmatte (553)	SP
OTER1	Otterbach (500)	BB, SM
OTER2	Otterbach (2,740)	SP
Nagra network		
SAIRA	Les Sairains Dessus	BB

Instrument type (all three-component): *SP* 1 s, *SM* accelerometer

The numbers in parentheses next to the borehole stations are the sensor depth with respect to ground surface in meters

In 2006 an array of seismic sensors was installed in six boreholes at depths between 317 and 2,740 m beneath Basel (e.g. Deichmann and Ernst 2009). This array was designed to monitor the seismicity induced by the injection of large quantities of water at high pressure into a 5 km deep well in the context of a project initiated by Geopower Basel AG, a private/public consortium, to extract geothermal energy. Except for station OTER1, the five-station borehole array is operated by Geothermal Explorers Ltd in Pratteln. At the beginning of 2011, four of these stations continued to operate, but in February, station HALTI failed and had to be abandoned.

The SED continues to maintain a micro-network originally deployed in 2005 in the region between the Lukmanier Pass and the Leventina Valley to monitor with greater precision an ongoing sequence of earthquakes in the immediate vicinity of the southern segment of the new Gotthard railway tunnel, which is still under construction. In 2011, the two stations inside the tunnel, PIORA and MFSFA, were removed, and a new broadband surface station (NALPS) was installed at the end of October to the north at Lai di Nalps, closer to the zone of active tunneling. Operation of the network was funded until March 31st, 2011, under a contract with AlpTransit-Gotthard AG. After

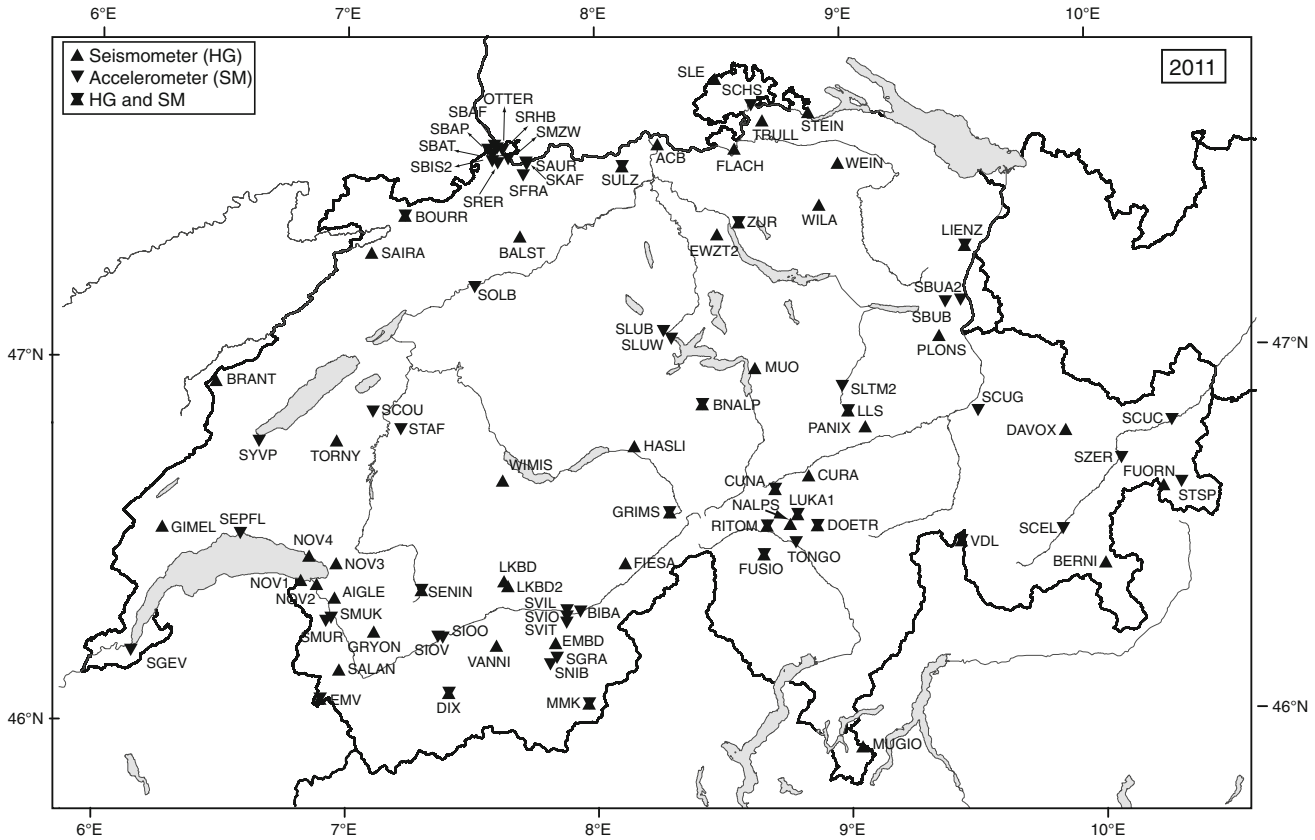

Fig. 1 Seismograph stations in Switzerland with on-line data acquisition operational at the end of 2011. The stations defined as high-gain (HG) are mostly equipped with broad-band or 5-s sensors, whereas the strong-motion stations (SM) are accelerometers. For a map of the Basel-borehole array see Baer et al. (2007) or Deichmann and Ernst (2009)

that date, SED continued to operate the stations at its own expense for the rest of the year.

The earthquakes induced by the geothermal project in Basel have raised concerns about potential seismicity induced by other geothermal projects (even those that do not involve the enhancement of permeability through massive water injections). Therefore, it has become common practice to include local monitoring capabilities for such projects. The four-station array around the southeast tip of Lake Geneva associated to a project near Noville, drilling for natural gas, continued to be operated through 2011.

A long term project to monitor seismicity down to magnitude M_L 1.0 across north-eastern Switzerland began in 2011. This project, under a contract with the National Cooperative for the Disposal of Radioactive Waste (NAGRA), aims at detection and characterization of small, seismically active faults in the area of candidate sites for deep nuclear waste repositories. In order to reach these goals, the number of stations in the region will be increased substantially by installing eight additional broadband surface stations and two short-period borehole stations at a depth of 125 m in northern Switzerland and southern Germany. In 2011, the station SAIRA was installed as part of this project.

To improve the reliability of locations for events at the periphery or outside of Switzerland, we continue to be engaged in an ongoing cross-frontier cooperative effort to exchange seismic data in realtime. We continuously record and archive signals from stations in Austria operated by the Zentralanstalt fur Meteorologie und Geodynamik in Vienna (ZAMG) and in Italy operated by the Istituto Nazionale di Geofisica e Vulcanologìa in Rome (INGV), by Istituto di Geofisica, Università di Genova, the Zivilschutz der Autonomen Provinz Bozen-Südtirol (Baer et al. 2007), the Istituto Nazionale di Oceanografia e di Geofisica Sperimentale (OGS) in Trieste, and in Germany by the Landeserdbebendienst Baden-Württemberg in Freiburg. In 2011, we began receiving data in realtime also from the Reseau Sismologique et Géodésique Français (RESIF) in France, including, for the first time, a foreign strong-motion station. A total of 29 foreign stations were monitored at the SED in 2011, and the number continues to increase as new high-quality stations come on-line in the border region.

2.2 Hypocenter location, magnitude and focal mechanisms

Since 2005, hypocenter locations of most of the local earthquakes have been determined using the software package NonLinLoc (Lomax et al. 2000). The P-wave velocity model was derived from a 3D tomographic inversion of local earthquake data with constraints from controlled source seismics (Husen et al. 2003), and the S-velocities were calculated from the P-velocity using a Vp/Vs ratio of 1.71.

Local magnitudes (M_L) are calculated from the maximum amplitude of the horizontal components of the digital broad-band seismograms filtered to simulate the response of a Wood-Anderson seismograph. The attenuation with epicentral distance is accounted for by an empirically determined relation (Kradolfer and Mayer-Rosa 1988). The final magnitude corresponds to the median value of all individual station magnitudes. For the stronger events, the traditional determination of focal mechanisms from the azimuthal distribution of first-motion polarities (fault-plane solutions) is complemented by moment tensors based on full-waveform inversion. This procedure, based on a time domain inversion scheme developed by Dreger (2003), also provides a moment magnitude, M_w, the best fitting double couple, and an optimal depth estimate based on the given location. Recently an additional procedure has been implemented that routinely and automatically provides estimates of M_w also for earthquakes of lower magnitudes. M_w values are computed using a spectral fitting technique following the method of Edwards et al. (2010). The far-field signal moments are obtained by simultaneously fitting the spectrum of a theoretical source model (Brune 1970, 1971) along with path variable attenuation and event stress-drop to observed Fourier velocity spectra. The seismic moment is derived from the far-field signal moments assuming a simple geometrical spreading model that accounts for body and surface wave propagation. Site amplification is assumed negligible for the computation of M_w due to the predominant use of hard-rock recording sites (Poggi et al. 2011).

A more detailed documentation of the data analysis can be found in previous annual reports, particularly Deichmann et al. (2006) and Baer et al. (2007).

3 Seismic activity during 2011

3.1 Overview

During 2011, the Swiss Seismological Service detected and located 522 earthquakes in the region shown in Fig. 2. Based on criteria such as the time of occurrence, location, signal character or on direct communication, 92 additional seismic events were identified as quarry blasts.

Magnitude values of the events recorded in 2011 range from M_L 0.1 to 3.3 (Fig. 3). The events with $M_L \geq 2.5$ and the criteria, used to assign the quality rating for the given locations as well as the corresponding estimated location accuracy, are listed in Tables 4, 5. Table 4 also includes the available M_w values derived from the spectral fitting method of Edwards et al. (2010). Fault-plane solutions based on first-motion polarities are shown in Fig. 4 and their parameters are listed in Table 6.

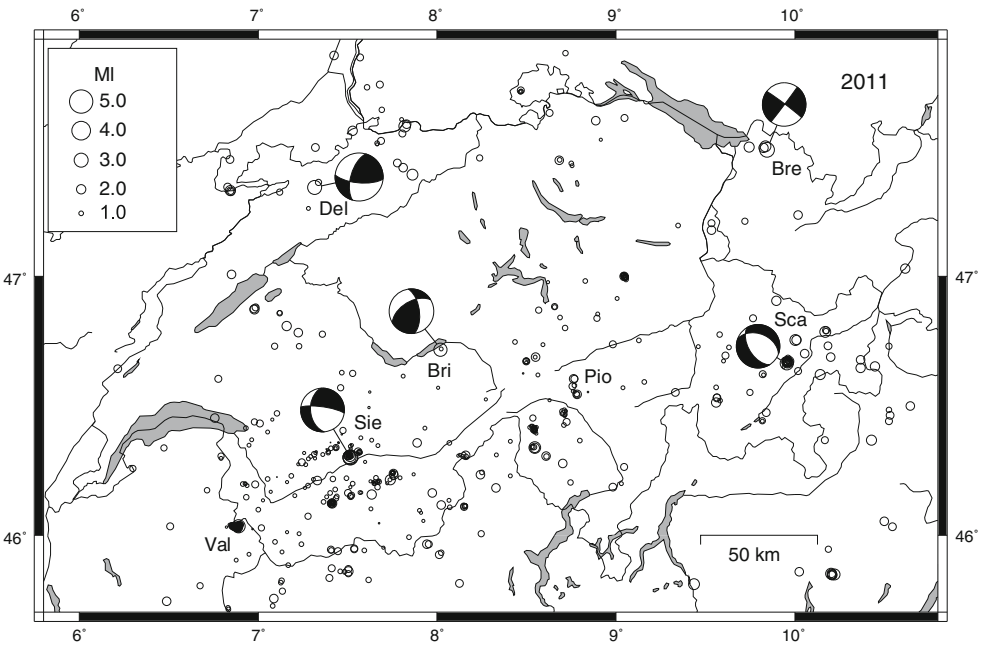

Fig. 2 Epicenters and focal mechanisms of earthquakes recorded by the Swiss Seismological Service during 2011. Epicenters of events mentioned in the text are Bregenz (Bre), Brienz (Bri), Delémont (Del), Piora (Pio), Scalettapass (Sca), Sierre (Sie), and Vallorcine (Val). Magnitudes as well as focal depths are listed in Table 4, and focal mechanism paramaters in Table 6

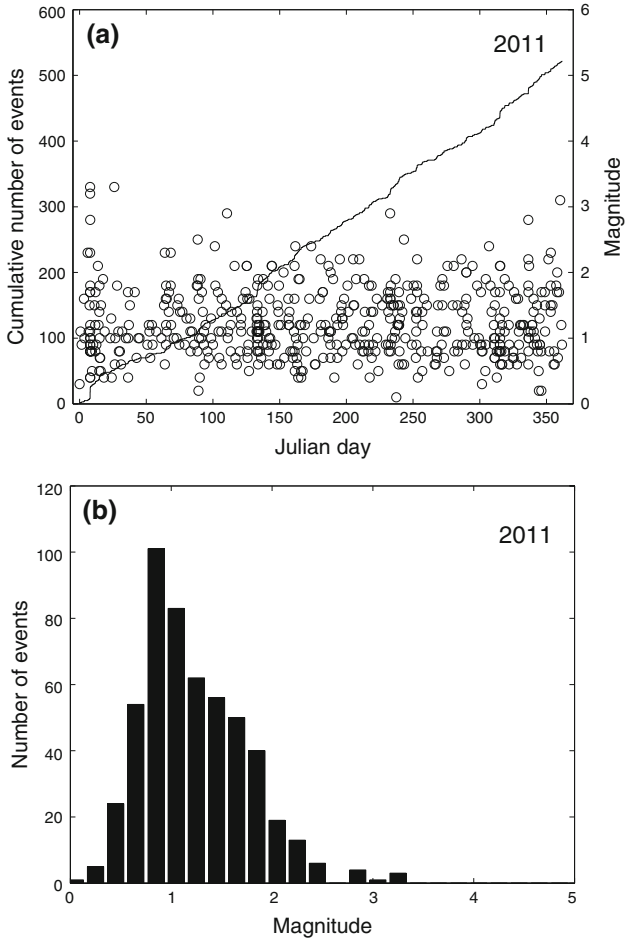

Fig. 3 Earthquake activity during 2011 **a** magnitude of each event and cumulative number of events, **b** histogram of magnitudes. See also Table 4

Figure 5 shows the epicenters of the 880 earthquakes with $M_L \geq 2.5$ which have been recorded in Switzerland and surrounding regions over the period 1975–2011. These events represent about 8 % of the total number of events detected during that time period in the same area. The chosen magnitude threshold of M_L 2.5 ensures that the data set is complete for the given period and that the number of unidentified quarry blasts and of badly mislocated epicenters is negligible.

3.2 Significant earthquakes of 2011

3.2.1 Sierre

The earthquake sequence of Sierre represents the most significant seismic activity of 2011 in Switzerland (for location see Fig. 2). It comprises a total of 31 events with M_L between 0.4 and 3.3, and began January 8th at 20:28 UTC with an event of M_L 2.3. As shown in Fig. 6, 16 events occurred in the first 5 h and included two events of M_L 3.3 and 3.2. An additional nine events occurred over the following 2 weeks; then the sequence continued with sporadic events until the end of the year. The epicenter of the main shock was located about 2 km NW of the town of Sierre, and the focal depth of 6–7 km is well constrained by records at two accelerographs located at epicentral distances of 3 and 8 km. This focal depth also agrees with 2-D ray-trace modeling of travel-time differences between the reflection at the Moho, PmP, the direct wave, Pg, and the refraction in the upper mantle, Pn, observed at stations in NE Switzerland.

The fault-plane solutions of the two strongest events are well constrained and are very similar to each other (Fig. 7, Table 6). Given that the signals of the individual events are very similar, it was possible to apply a time-domain cross-correlation procedure to determine high-precision arrival-time differences and thus precise hypocenter locations relative to a chosen master event. The cross-correlation procedure documented in Deichmann and Garcia-Fernandez (1992) was applied to the seismograms of the first 24

Table 4 Earthquakes with $M_L \geq 2.5$

Date and Time UTC	Lat. (°N)	Lon. (°E)	X/Y (km)	Z (km)	Mag. (M_L)	Mag. (M_w)	Q	Location
2011.01.08 20:48:17	46.304	7.516	606/128	7	3.3	3.0	A	Sierre, VS
2011.01.08 22:20:26	46.302	7.516	606/128	6	3.2	3.0	A	Sierre, VS
2011.01.08 23:32:30	46.304	7.510	605/128	7	2.8	2.7	A	Sierre, VS
2011.01.27 01:24:18	47.482	9.844	781/262	31	3.3	2.9	A	Bregenz, A
2011.03.30 13:01:12	47.572	7.818	629/269	13	2.5	2.4	A	Rheinfelden, AG
2011.04.21 11:36:39	46.719	8.019	644/174	7	2.9	2.7	A	Brienz, BE
2011.08.21 19:39:45	46.039	6.887	557/99	4	2.9	2.8	A	Vallorcine, F
2011.09.01 02:50:30	46.341	8.546	685/133	9	2.5	2.3	B	Bosco Gurin, TI
2011.12.03 08:32:52	46.666	9.955	792/171	9	2.8	2.8	A	Scaletta Pass, GR
2011.12.27 06:29:02	47.339	7.315	591/243	11	3.1	2.8	A	Delémont, JU

The values listed under M_w are the moment magnitudes calculated from the spectral fitting method documented in Edwards et al. (2010)

Table 5 Criteria and location uncertainty corresponding to the quality rating (Q) of the hypocentral parameters in the event list

Rating	Criteria		Uncertainty	
Q	GAP (degrees)	DM (km)	H (km)	Z (km)
A	≤180	≤1.5 × Z	≤2	≤3
B	≤200	≤25	≤5	≤10
C	≤270	≤60	≤10	>10
D	>270	>60	>10	>10

GAP largest angle between epicenter and two adjacent stations, *DM* minimum epicentral distance, *H* horizontal location, *Z* focal depth

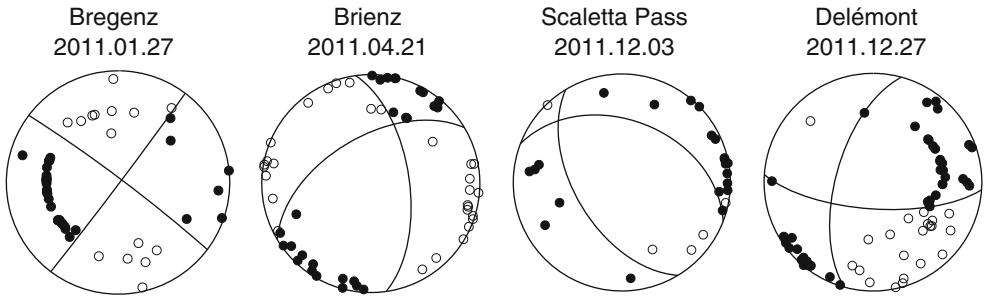

Fig. 4 Fault-plane solutions based on first-motion polarities. All stereographs are lower hemisphere, equal-area projections. *Solid circles* correspond to compressive first motion (*up*); *empty circles* correspond to dilatational first motion (*down*). The corresponding parameters are listed in Table 6

Table 6 Focal mechanism parameters based on first-motion polarities (cf. Figs. 2, 4, 7)

Location	Date and Time (UTC)	Depth (km)	Mag.	Plane 1 Strike/Dip/Rake	Plane 2	P-Axis Azimuth/Dip	T-Axis
Sierre	2011/01/08 20:48	7	M_L 3.3	278/78/-133	175/44/-017	148/41	039/21
Sierre	2011/01/08 22:20	6	M_L 3.2	268/85/-141	174/51/-006	138/30	034/22
Bregenz	2011/01/27 01:24	31	M_L 3.3	037/89/003	307/87/179	172/01	262/03
Brienz	2011/04/21 11:36	7	M_L 2.9	352/61/041	239/55/144	114/04	208/48
Scaletta Pass	2011/12/03 08:32	9	M_L 2.8	291/42/-120	149/55/-066	114/69	222/07
Delemont	2011/12/27 06:29	11	M_L 3.1	094/70/150	195/62/023	146/05	052/35

events of the sequence, recorded at six stations. It relies on a least-squares adjustment of travel-time differences computed for all possible combinations of event pairs. As master event we chose the first event of the sequence (M_L 2.3). Because of the large difference in the dominant frequency of the strongest and weakest events, which tends to impair the reliability of the cross-correlations, the correlations were performed separately, first for the master event and the three largest events and then for the master event and all the smaller events. Relative locations based on the resulting travel-time differences of five P and four S arrivals were computed with the method proposed by Console and Di Giovambattista (1987). For the subset of the larger events, it was possible to use also arrival-time differences of the phases reflected at the Moho (PmP) recorded at stations ZUR and CURA, which add a valuable constraint on the relative focal depths of these events. With mean relative travel-time errors of 3–6 ms, estimated from the cross-correlations and mean residuals of 1–6 ms resulting from the location procedure, we obtain relative location uncertainties of 7–10 m horizontally and 22–40 m vertically (single standard deviations). As shown in Fig. 7, the hypocenters of the 2011 Sierre sequence delineate two separate E–W striking fault segments that are parallel to one of the nodal planes of the fault-plane solution. Thus, the focal mechanism of the Sierre events corresponds to dextral strike-slip with a strong vertical component of slip along an almost vertical E–W striking fault. Noteworthy is the fact that the Sierre sequence is located at the northern edge of the Rhone Valley and is not part of the pronounced lineament further to the north that strikes WSW-ENE and that has been active for several decades. Its focal

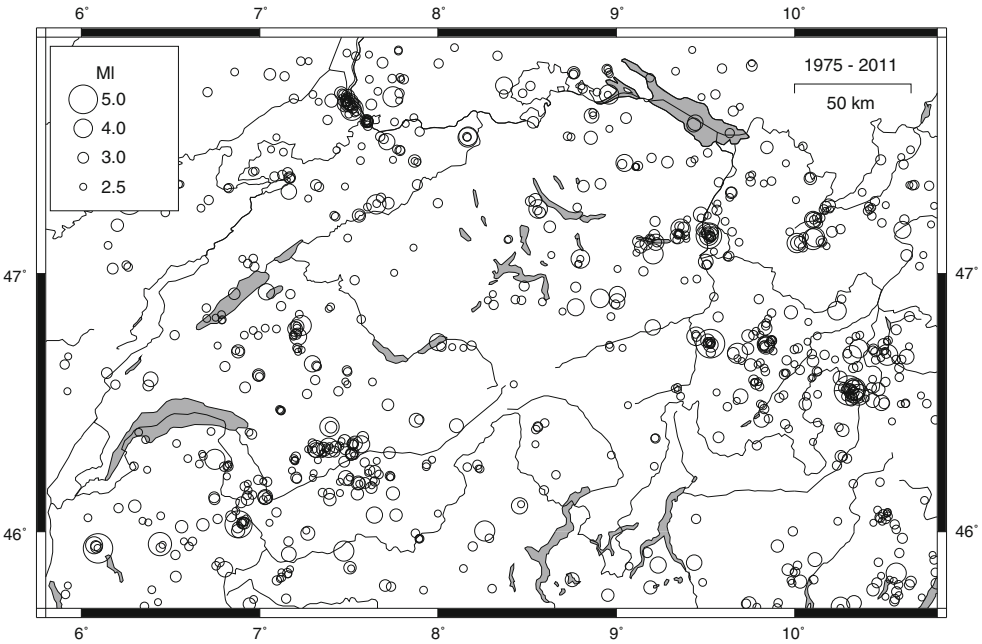

Fig. 5 Epicenters of earthquakes with Magnitudes $M_L \geq 2.5$, during the period 1975–2011

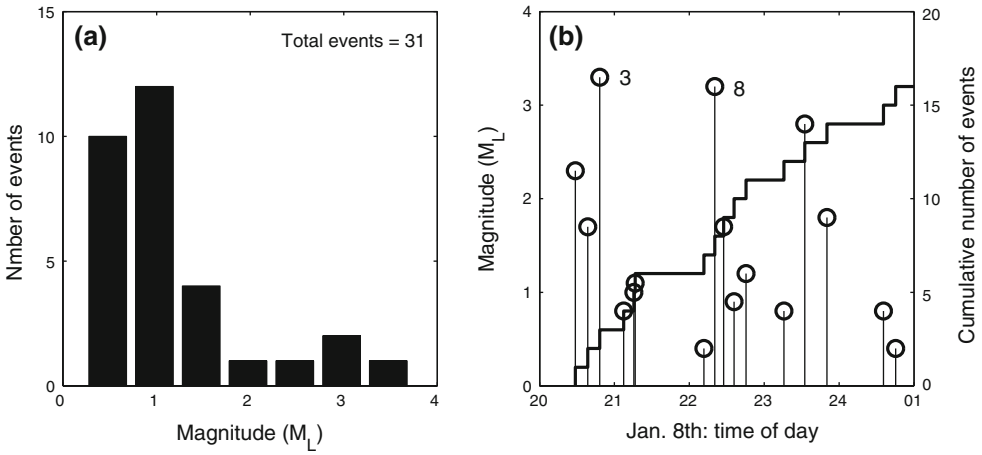

Fig. 6 Statistics of the sequence of Sierre (for location see Fig. 2) **a** magnitude histogram (M_L) of all events recorded in 2011, **b** magnitude of each event and cumulative number of events as a function of time during the first 5 h of the sequence. The events are numbered consecutively (see also Fig. 7) 3 and 8 are the two strongest events, with M_L 3.3 and 3.2. Focal mechanisms and macroseismic intensities of these two events are shown in Figs. 7, 8

mechanism with the strong oblique component of slip is also not typical of either the strike-slip mechanisms that characterize the seismicity in the Helvetic domain of the northern Wallis nor of the normal faulting mechanisms that predominate in the Penninic nappes of the southern Wallis (Maurer et al. 1997; Kastrup et al. 2004).

The two strongest events (M_L 3.3, 3.2) caused shaking of intensity IV (EMS-98) in the epicentral region and were felt over large parts of the Canton Wallis and in parts of the Berner Oberland (Fig. 8). Even the M_L 2.8 event was felt by the local population. Table 7 lists peak ground velocities (PGV) and peak ground accelerations (PGA) of the two strongest events recorded at selected stations close to the epicenters. It is noteworthy that both PGV and PGA at the two closest stations (Sierre and Ayent) are higher by almost a factor of 2 for the second event than for the first, despite the fact that M_w is the same for both events and that M_L of the first one is even slightly larger than that of the second one. The difference in the measured PGV and PGA values is reflected also in the macroseismic observations: although the second event occurred later at night and the shaking at larger distance seems not to have been sufficiently strong to wake people up, the reports from people in the immediate epicentral region indicate clearly that the shaking was more intense for the second event.

3.2.2 Bregenz

The M_L 3.3 earthquake that occurred January 27th near Bregenz, at the north-eastern end of the Bodensee, is noteworthy because of its focal depth. The depth of 31 km is well constrained by P and S-onsets at three stations at epicentral distances between 22 and 34 km. According to Waldhauser et al. (1998) the Moho lies at a depth of

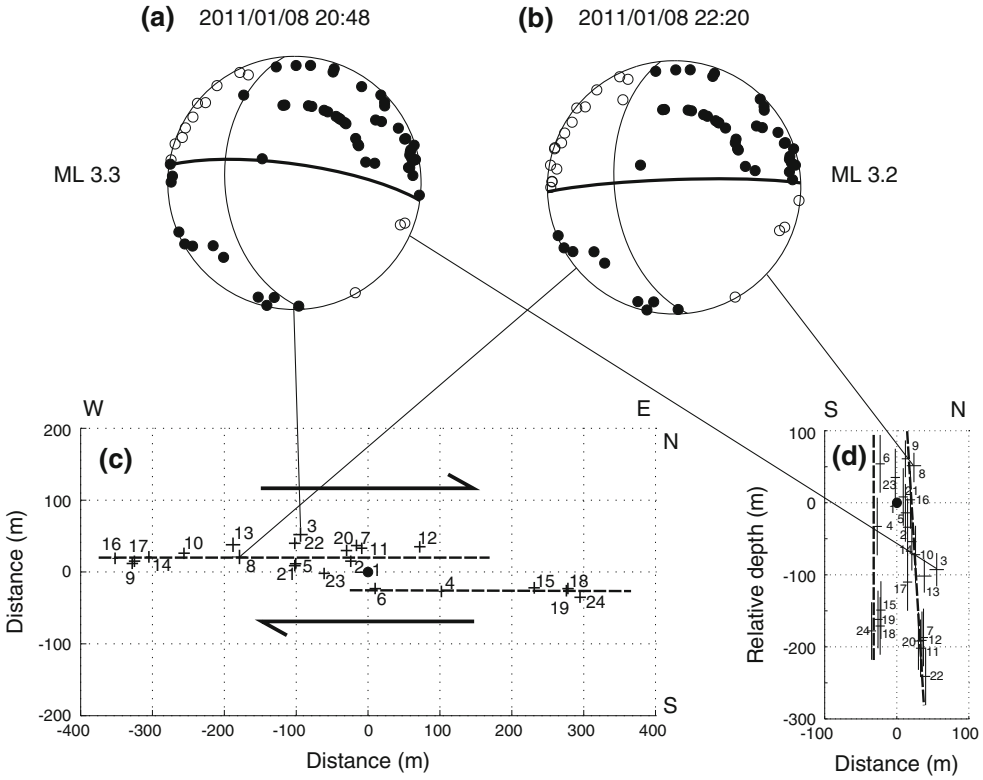

Fig. 7 The earthquake sequence of Sierre (for location see Fig. 2) **a** and **b** fault-plane solutions of the two strongest events (# 3 and 8), **c** epicenter locations (map view) and **d** depth cross-section relative to the chosen master event (# 1). In **c** and **d** the events are numbered consecutively with time, and the *dashed lines* delineate the inferred fault planes. The *arrows* in **c** indicate the sense of slip

34–35 km at this location. Consequently, as can be seen in Fig. 9, at stations located in the Alpine foreland to the west of the epicenter, the wave refracted at the Moho (Pn) appears as the first arrival already at a distance of about 70 km. Note that the time scale in Fig. 9 has been shifted by subtracting the epicentral distance divided by a reduction velocity of 6.4 km/s. The fact that beyond about 120 km the secondary arrivals lie on a horizontal line implies that the average P-wave velocity in the lower crust below the northern Alpine foreland is probably not higher than 6.4 km/s. Given the large focal depth and the fact that it occurred in the middle of the night, it is not surprising, that it was noticed only by very few persons. Two additional events with practically identical hypocenter locations occurred March 10th and May 25th with M_L 2.3 and 2.1.

The fault-plane solution corresponds to a strike-slip mechanism with NE–SW and NW–SE striking nodal planes (Figs. 2, 4). The former is well constrained by the available first-motion data, while the latter is constrained by the fact that the amplitude of the Pn phase recorded at station BFO, located at a distance of 147 km and an azimuth of 309 degrees, is so weak that the location of this station must coincide with the strike of the NW–SE nodal plane. The resulting focal mechanism and the focal depth are almost identical to those of the M_L 3.0 event that occurred April 18th 2004 near Lindau, about 7 km to the NW of Bregenz.

3.2.3 *Brienz*

The focal depth of 7 km of the M_L 2.9 earthquake that occurred April 21st just south of Brienz is constrained by P and S-arrivals at station HASLI, at an epicentral distance of 11 km, and by several Pn arrivals at stations in southern Germany. The fault-plane solution, shown in Fig. 4, corresponds to a thrust mechanism with a strong strike-slip component. The almost horizontal P-axis is oriented in a NNW-SSE direction (Table 6), which is typical of the seismic deformation observed in the Helvetic domain of central Switzerland (Kastrup et al. 2004). There is no evidence that this event was felt.

3.2.4 *Vallorcine*

As in previous years (e.g. Deichmann et al. 2011), the aftershock activity of the M_L 4.9 earthquake that occurred in 2005 near Vallorcine, between Martigny and Chamonix, just south of the border with France (Fréchet et al. 2010), continued throughout the year 2011. A total of 48 aftershocks with magnitudes between M_L 0.4 and 2.9 were recorded in 2011.

3.2.5 *Scaletta Pass*

The M_L 2.8 event of December 3rd with epicenter located 11 km ENE of Zernez was the second event of a sequence

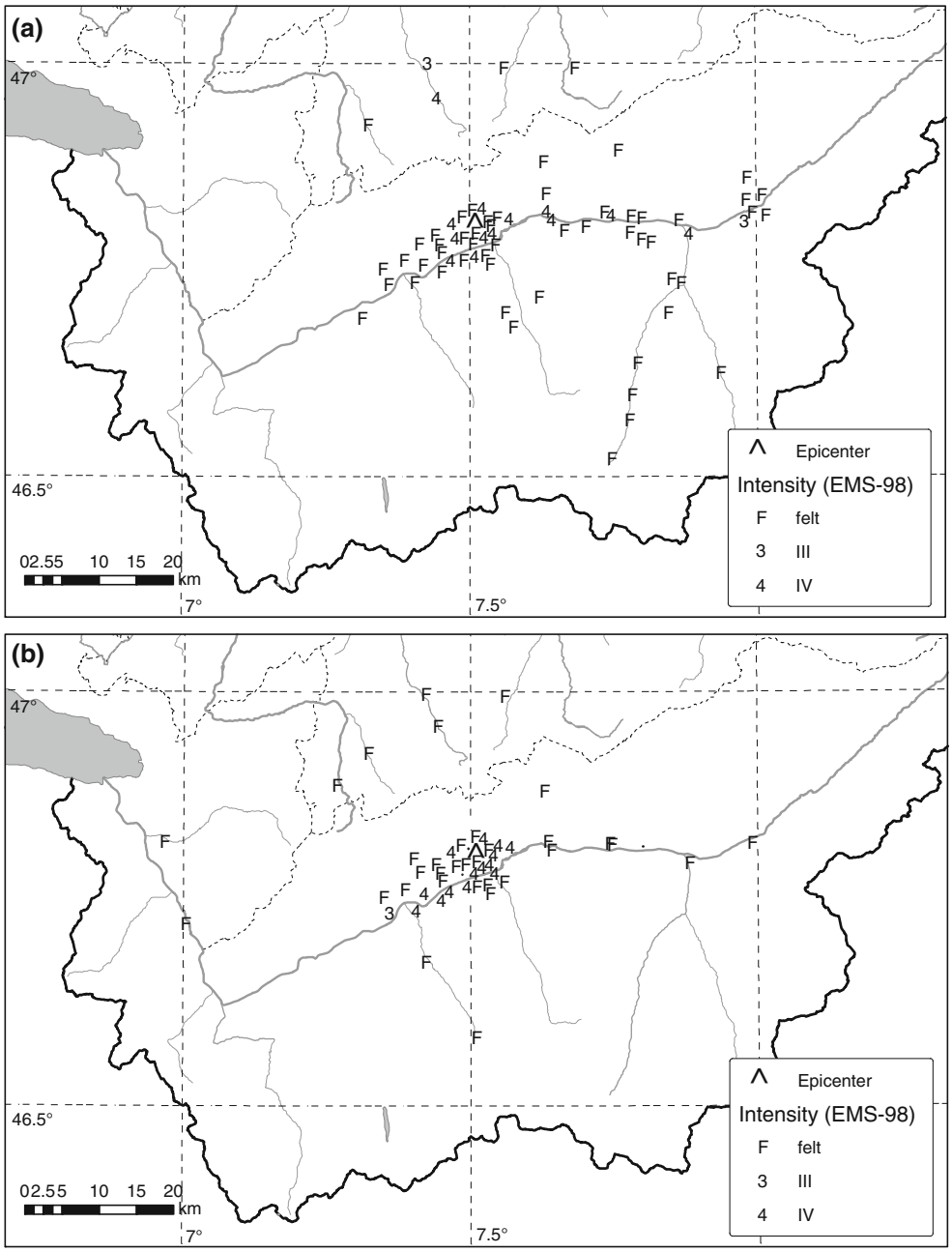

Fig. 8 Macroseismic intensities (EMS98) of the two strongest events of the sequence of Sierre **a** 2011/01/08, 21:48 local time, M_L 3.3 and **b** 23:20 local time, M_L 3.2

that started November 29th. The focal depth of 9 km is constrained only by P and S-arrivals recorded at stations SZER and DAVOX at epicentral distances of 11 and 14 km. However, this focal depth is within the depth range of most well-located earthquakes in south-eastern Switzerland. The normal faulting focal mechanism of this event, shown in Fig. 4, is very similar to that of the nearby Sertig sequence of 2005 and constitutes further evidence for the predominantly extensional deformation of this region (Marschall et al. in press). This event was felt very mildly by a few people in the Lower Engadine.

3.2.6 Delémont

The earthquake that occurred December 27th at 7:29 in the morning (local time) was the fourth and last event with $M_L > 3$ of the year 2011. Its epicenter was located near the village of Courtételle, about 3 km south-west of Delémont,

Table 7 Peak ground velocity (PGV, mm/s) and peak ground acceleration (PGA, mm/s^2) recorded at selected locations for the two strongest events of the earthquake sequence of Sierre

2011.01.08			20:48 (M_L 3.3)			22:20 (M_L 3.2)		
STAT	LOCATION	DIST	RSH	PGV	PGA	RSH	PGV	PGA
SIES	Sierre-Solaire	3.1	0.363	2.17	122.	0.330	4.05	201.0
SAYF	Ayent-Fortunoz	7.9	−0.866	1.41	80.0	−0.970	2.79	153.0
VANNI	Vissoie	12.1	0.393	0.384	10.8	0.524	0.358	11.7
SIOO	Sion-Ophtalm.	13.1	−0.316	0.420	12.1	−0.491	0.412	16.2
SIOM	Sion-Mayennaz	14.7	−0.353	0.168	7.23	−0.533	0.205	9.72
SENIN	Sanetsch	17.8	−0.633	0.212	9.19	−0.565	0.211	10.1

DIST is the epicentral distance in km and RSH is the radiation coefficient of the SH wave for each focal mechanism. PGV and PGA were determined from horizontal records rotated to maximize the absolute value of the peak amplitudes

and the focal depth of 11 km is constrained by P and S-arrivals at station BOURR, 9 km from the epicenter, as well as by several Pn arrivals at stations in southern Germany and south-eastern Switzerland. There are no credible reports of this earthquake having been felt.

The fault-plane solution corresponds to a strike-slip mechanism with a slight thrust component (Figs. 2, 4). It hinges to a very large degree on the first motion at ECH, the point on the northern edge of the nodal plane that strikes almost north–south and dips towards the west in Fig. 4. The first motion at this station is unequivocally "up", as illustrated in Fig. 10. Given that ECH is located at an epicentral distance of only 98 km, it is less obvious that it is a Pn rather than a Pg phase. However, several observations support this interpretation: (a) the amplitude is low compared to the subsequent phases, which is what one would expect from the Pn at distances close to the cross-over distance between Pn and Pg; (b) in a plot of travel-time versus epicentral distance, its arrival-time, reduced with a velocity of 6.0 km/s, is much earlier than the Pg at station MOF at the same azimuth, and slightly earlier than the Pg observed at stations END, KIZ and FELD located in the Black Forest; (c) ray-trace calculations with a simple 2D crustal model confirm that, for a focal depth of 11 km and a Moho depth that varies between 28 and 25 km, the cross-over distance is indeed around 100 km; and (d) interpreting this phase with a positive polarity as a Pg results in an inconsistent fault-plane solution.

Previously in 2010, another small earthquake (M_L 2.8) occurred near the town of Courtételle, only 1–2 km ESE of

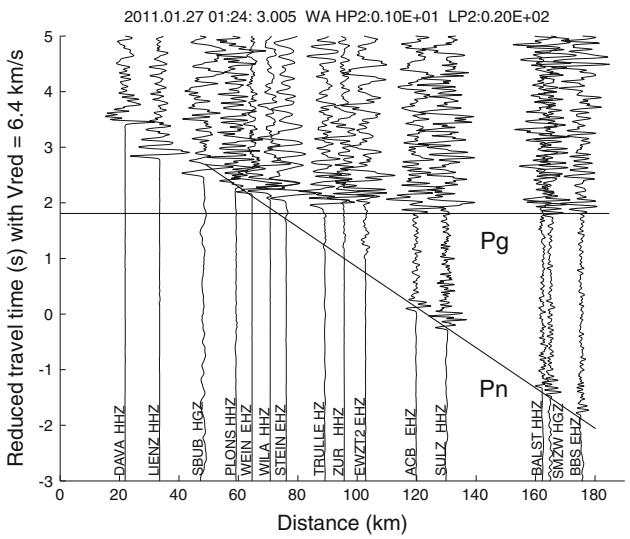

Fig. 9 Record-section with seismograms of the Bregenz event, recorded at stations located to the west of the epicenter (within ± 10 degrees). Note that the time scale has been reduced with a velocity of 6.4 km/s

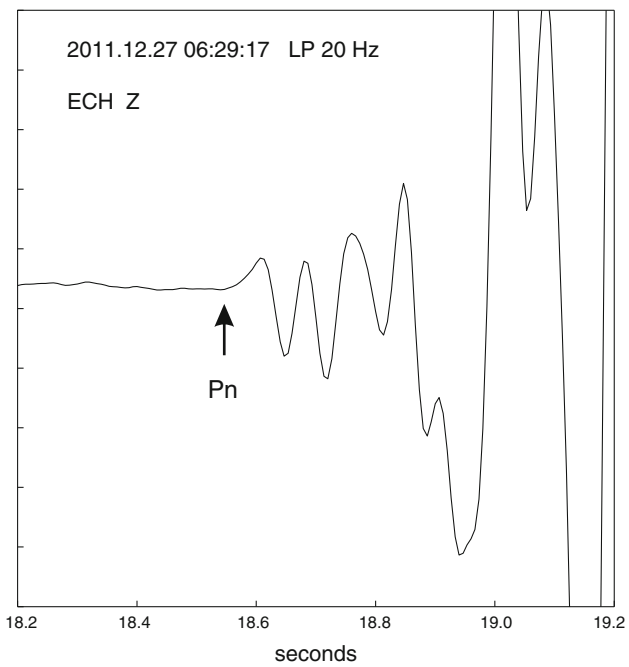

Fig. 10 Seismogram of the Delémont event recorded at station ECH (France): the first arrival is the phase refracted at the Moho (Pn), with upward first-motion. The signal is filtered with a 2nd order causal Butterworth low-pass filter at 20 Hz

the Delémont event. However, with a focal depth of 18 km, the hypocenter of the former was substantially deeper (Deichmann et al. 2011), as was verified by a comparison of the Pn/Pg crossover distances of these two events.

3.2.7 Piora

During 2011, the AlpTransit network recorded 46 earthquakes with local magnitudes between 0.2 and 1.8 in the Piora region. Of these, 33 earthquakes could be located. The remaining earthquakes were too small and mostly recorded only at station PIORA, but 9 earthquakes were strong enough to be detected by the SDSNet. Their computed epicenter locations coincide to within a few hundred meters with the trace of the Gotthard base-tunnel, which was under construction at that time. Computed focal depths vary between 1 and 2 km for the five events at minimum epicentral distances of 1–3 km (station PIORA) and between 2 and 4 km for the four events further north at minimum distances of 5 km (station CUNA). The true focal depths are probably even shallower, as the regional 3-D P-wave velocity model used for location may not be appropriate at such a small scale. In a similar setting further south along the tunnel, near the town of Faido, routinely calculated focal depths were also found to be deeper than those determined using a velocity model that was refined based on a calibration shot (Husen et al. 2011). Compared to previous years, we observe an overall northward migration of the epicenters, in general accord with the northward extension of the ongoing tunnel excavation.

3.3 Landslides

In 2011, the national network detected 13 events that are suspected to be landslides or rock avalanches. This could be confirmed for six of these events: Bäregg near Grindelwald, Les Drus near Chamonix (four events) and Pizzo Cengalo, between Maloja and Chiavenna.

The Bäregg event occurred September 6th at 22:35 UTC. Its confirmation is based only on acoustic evidence reported by a local resident. It is possible that this event was caused by slope failure in the east flank of Eiger, similar to the events that occurred there in 2006 (Baer et al. 2007).

The four detected rock avalanches near Chamonix, France, occurred September 11th, 08:14, September 12th, 05:39 and 05:43 as well as October 30th, 06:12 UTC. These four events were caused by renewed slope failures on the west face of the Aiguille du Petit Dru. Similar events have also been detected in 1997 (Deichmann et al. 1998). Equivalent magnitudes could be computed for the first and last of these events (M_L 1.5 and 1.8). As shown in Fig. 11, the first is particularly interesting, because, embedded in the usual emergent wave-train, it produced highly impulsive signals that could be interpreted as P and S-waves, resulting in an epicenter location that coincides within less than 1 km with the location of the documented rock avalanche. The impulsive signals are probably due to the impact of a large rock mass on the ground at the foot of the near-vertical west face.

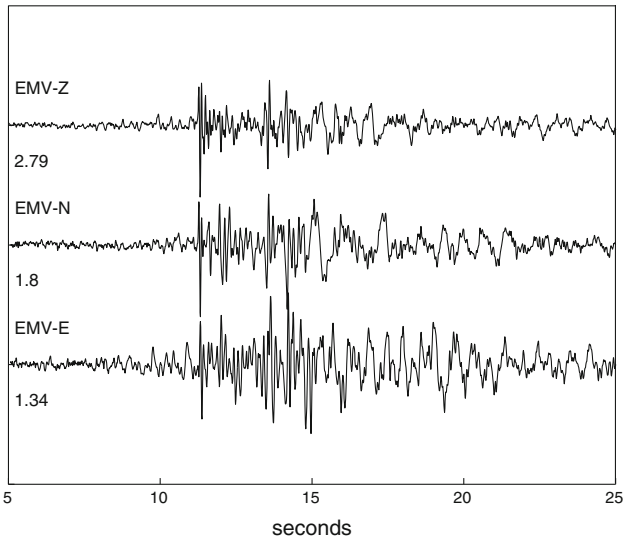

Fig. 11 Seismograms of the first detected rock-fall from the west face of Les Drus near Chamonix, France, recorded at station EMV (Emosson), at a distance of 15 km. The signals are filtered with a 2nd order causal Butterworth band-pass filter between 1 and 20 Hz. Note the higher-frequency signal with impulsive P and S-arrivals embedded in the emergent and longer-lasting signal, typical for a landslide

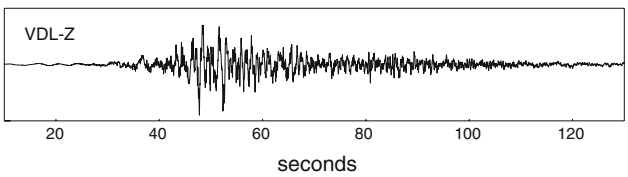

Fig. 12 Seismogram of the massive landslide from Pizzo Cengalo, Val Bregaglia, December 27th, 2011, recorded at station VDL (Valle di Lei), 24 km away. The signal is filtered with a 4th order zero-phase Butterworth band-pass filter between 0.2 and 20 Hz. Note the time scale: the entire seismogram is nearly 2 min long

The largest landslide occurred on December 27th, at 17:25 UTC, as part of a sequence of events associated with a massive slope failure in the north face of Pizzo Cengalo at the head of Val Bondasca, on the border with Italy. With an equivalent magnitude of M_L 2.7, it was recorded over the entire Swiss national network and was even detected by the German Regional Seismic Network. As shown in Fig. 12, the vibrations caused by this event lasted nearly 2 min.

In the context of a PhD project at the Department of Earth Sciences at ETH Zurich, procedures are being

developed to automatically identify landslides and massive rock avalanches, and to estimate their volume based on their seismic signals. First results based on a previous master thesis have been published in Dammeier et al. (2011).

4 Discussion

In 2011, as in previous years, a large portion of the seismic activity was concentrated in the Valais and the immediately adjacent regions. Compared to the relative low of the year before, seismic activity in Graubünden returned to more normal levels, while the activity observed since 2008 in the region around the upper Valle Maggia continued with several small events. Routinely calculated focal depths for all but 12 events recorded in 2011 are less than 16 km. All of the deeper hypocenters occurred below the Molasse Basin and Jura of northern Switzerland and southern Germany. The seismic activity, induced by the geothermal project in Basel in 2006 and 2007 (e.g. Deichmann and Ernst 2009; Deichmann and Giardini 2009), continued to decrease over the year 2011, and all events that have been recorded by the local borehole seismometers were too weak to be recorded by the national broad-band network. Overall, the seismic activity in and around Switzerland was low in 2011, both in terms of the number of events and in terms of the maximum event magnitude. The total number of 10 events with $M_L \geq 2.5$ is substantially below the yearly average of about 24 events over the previous 36 years in this magnitude range and is the lowest since 1975, the beginning of the Swiss instrumental earthquake catalog. The M_L 3.3 is also the lowest maximum magnitude per calender year since 1981.

Acknowledgments Monitoring the seismicity in a small country is not possible without international cooperation. We thank W. Brüstle and S. Stange of the Erdbebendienst des Landesamtes für Geologie, Rohstoffe und Bergbau Baden-Württemberg in Freiburg (LGRB), who kindly responded to our requests for information and data in 2011. Automatic data exchange in real-time has been implemented with LGRB, with the Zentralanstalt für Meteorologie und Geodynamik in Vienna, with the Istituto Nazionale di Geofisica e Vulcanologìa in Rome and with the Zivilschutz der Autonomen Provinz Bozen-Südtirol. Access to the data of the borehole sensors in Basel was granted by Geopower Basel AG, and we thank Geothermal Explorers Ltd for their help. We are also very grateful to P. Zweifel and our colleagues in the SED electronics lab for their relentless efforts in ensuring the continuous reliability of the data acquisition systems, and to E. Läderach, S. Räss and A. Blanchard for administrative and logistic support. Financial support from the Nationale Genossenschaft für die Lagerung radioaktiver Abfälle, Nagra, for the operation of several stations in northern Switzerland, as well as from AlpTransit-Gotthard AG for the operation of the network around the southern segment of the new Gotthard Tunnel is gratefully acknowledged. Installation and operation of the Noville network are funded under a contract with Petrosvibri S.A.

References

Baer, M., Deichmann, N., Fäh, D., Kradolfer, U., Mayer-Rosa, D., Rüttener, E., et al. (1997). Earthquakes in Switzerland and surrounding regions during 1996. *Eclogae Geologicae Helvetiae, 90*(3), 557–567.

Baer, M., Deichmann, N., Ballarin Dolfin, D., Bay, F., Delouis, B., Fäh, D., et al. (1999). Earthquakes in Switzerland and surrounding regions during 1998. *Eclogae Geologicae Helvetiae, 92*(2), 265–273.

Baer, M., Deichmann, N., Braunmiller, J., Ballarin Dolfin, D., Bay, F., Bernardi, F., et al. (2001). Earthquakes in Switzerland and surrounding regions during 2000. *Eclogae Geologicae Helvetiae, 94*(2), 253–264.

Baer, M., Deichmann, N., Braunmiller, J., Bernardi, F., Cornou, C., Fäh, D., et al. (2003). Earthquakes in Switzerland and surrounding regions during 2002. *Eclogae Geologicae Helvetiae Swiss J Geosci, 96*(2), 313–324.

Baer, M., Deichmann, N., Braunmiller, J., Husen, S., Fäh, D., Giardini, D., et al. (2005). Earthquakes in Switzerland and surrounding regions during 2004. *Eclogae Geologicae Helvetiae Swiss J Geosci, 98*(3), 407–418. doi:10.1007/s00015-005-1168-3.

Baer, M., Deichmann, N., Braunmiller, J., Clinton, J., Husen, S., Fäh, D., et al. (2007). Earthquakes in Switzerland and surrounding regions during 2006. *Swiss J Geosci, 100*(3), 517–528. doi: 10.1007/s00015-007-1242-0.

Brune, J. N. (1970). Tectonic stress and the spectra of seismic shear waves from earthquakes. *J Geophys Res, 75*, 4997–5010.

Brune, J. N. (1971). Correction: Tectonic stress and the spectra of seismic shear waves from earthquakes. *J Geophys Res, 76*, 5002.

Console, R., & Di Giovambattista, R. (1987). Local earthquake relative location by digital records. *Phys Earth Planet In, 47*, 43–49.

Dammeier, F., Moore, J. R., Haslinger, F., & Loew, S. (2011). Characterization of alpine rockslides using statistical analysis of seismic signals. *J Geophys Res, 116*, F04024. doi: 10.1029/2011JF002037.

Deichmann, N. (1990). Seismizität der Nordschweiz, 1987–1989, und Auswertung der Erdbebenserien von Günsberg, Läufelfingen und Zeglingen. *Nagra Technischer Bericht, NTB 90-46,* Nagra, Baden.

Deichmann, N., Baer, M., Ballarin Dolfin, D., Fäh, D., Flück, P., Kastrup, U., et al. (1998). Earthquakes in Switzerland and surrounding regions during 1997. *Eclogae Geologicae Helvetiae, 91*(2), 237–246.

Deichmann, N., Baer, M., Braunmiller, J., Ballarin Dolfin, D., Bay, F., Delouis, B., et al. (2000a). Earthquakes in Switzerland and surrounding regions during 1999. *Eclogae Geologicae Helvetiae, 93*(3), 395–406.

Deichmann N, Ballarin Dolfin D, Kastrup U (2000) *Seismizität der Nord- und Zentralschweiz. Nagra Technischer Bericht*, NTB 00-05, Nagra, Wettingen.

Deichmann, N., Baer, M., Braunmiller, J., Ballarin Dolfin, D., Bay, F., Bernardi, F., et al. (2002). Earthquakes in Switzerland and surrounding regions during 2001. *Eclogae Geologicae Helvetiae Swiss J Geosci, 95*(2), 249–261.

Deichmann, N., Baer, M., Braunmiller, J., Cornou, C., Fäh, D., Giardini, D., et al. (2004). Earthquakes in Switzerland and surrounding regions during 2003. *Eclogae Geologicae Helvetiae Swiss J Geosci, 97*(3), 447–458.

Deichmann, N., Baer, M., Braunmiller, J., Husen, S., Fäh, D., Giardini, D., et al. (2006). Earthquakes in Switzerland and surrounding regions during 2005. *Eclogae Geologicae Helvetiae Swiss J Geosci, 99*(3), 443–452. doi:10.1007/s00015-006-1201-1.

Deichmann, N., Baer, M., Clinton, J., Husen, S., Fäh, D., Giardini, D., et al. (2008). Earthquakes in Switzerland and surrounding

regions during 2007. *Swiss J Geosci, 101*(3), 659–667. doi:10.1007/s00015-008-1304-y.

Deichmann, N., Clinton, J., Husen, S., Haslinger, F., Fäh, D., Giardini, D., et al. (2009). Earthquakes in Switzerland and surrounding regions during 2008. *Swiss J Geosci, 102*(3), 505–514. doi:10.1007/s00015-009-1339-8.

Deichmann, N., Clinton, J., Husen, S., Edwards, B., Haslinger, F., Fäh, D., et al. (2010). Earthquakes in Switzerland and surrounding regions during 2009. *Swiss J Geosci, 103*(3), 535–549. doi:10.1007/s00015-010-0039-8.

Deichmann, N., Clinton, J., Husen, S., Edwards, B., Haslinger, F., Fäh, D., et al. (2011). Earthquakes in Switzerland and surrounding regions during 2010. *Swiss J Geosci, 104*(3), 537–547. doi:10.1007/s00015-011-0084-y.

Deichmann, N., & Ernst, J. (2009). Earthquake focal mechanisms of the induced seismicity in 2006 and 2007 below Basel (Switzerland). *Swiss J Geosci, 102*(3), 457–466. doi:10.1007/s00015-009-1336-y.

Deichmann, N., & Garcia-Fernandez, M. (1992). Rupture geometry from high-precision relative hypocenter locations of microearthquake clusters. *Geophys J Int, 110*, 501–517.

Deichmann, N., & Giardini, D. (2009). Earthquakes induced by the stimulation of an enhanced geothermal system below Basel (Switzerland). *Seismol Res Lett, 80*(5), 784–798. doi:10.1785/gssrl.80.5.784.

Dreger DS (2003) TDMT INV: time domain seismic moment tensor INVersion. In: WHK Lee, H Kanamori, PC Jennings, and C. Kisslinger (Eds.), *International Handbook of Earthquake and Engineering Seismology*, Academic Press, London (Part B, p. 1627).

Edwards, B., Allmann, B., Fäh, D., & Clinton, J. (2010). Automatic computation of moment magnitudes for small earthquakes and the scaling of local to moment magnitude. *Geophys J Int, 183*(1), 407–420. doi:10.1111/j.1365-246X.2010.04743.x.

Fäh, D., Giardini, D., Bay, F., Bernardi, F., Braunmiller, J., Deichmann, N., et al. (2003). Earthquake catalog of Switzerland (ECOS) and the related macroseismic database. *Eclogae Geologicae Helvetiae Swiss J Geosci, 96*(2), 219–236.

Fréchet, J., Thouvenot, F., Frogneux, M., Deichmann, N., & Cara, M. (2010). The M_w 4.5 Vallorcine (French Alps) earthquake of 8 September 2005 and its complex aftershock sequence. *J Seismol, 15*, 43–58. doi:10.1007/s10950-010-9205-8.

Giardini D, Wiemer S, Fäh D, Deichmann N, Sellami S, Jenni S and the Hazard Team of the Swiss Seismological Service (2004) *Seismic hazard assessment 2004 Swiss Seismological Service*, p. 81.

Husen, S., Kissling, E., Deichmann, N., Wiemer, S., Giardini, D., & Baer, M. (2003). Probabilistic earthquake location in complex three-dimensional velocity models: application to Switzerland. *J Geophys Res, 108*(B2), 2077–2096.

Husen, S., Kissling, E., & von Deschwanden, A. (2011). Induced seismicity during the construction of the Gotthard Base Tunnel, Switzerland: hypocenter locations and source dimensions. *J Seismol,*. doi:10.1007/s10950-011-9261-8.

Kastrup, U., Zoback, M.-L., Deichmann, N., Evans, K., Giardini, D., & Michael, A. J. (2004). Stress field variations in the Swiss Alps and the northern Alpine foreland derived from inversion of fault plane solutions. *J Geophys Res,*. doi:10.1029/2003JB002550 B01402.

Kastrup, U., Deichmann, N., Fröhlich, A., & Giardini, D. (2007). Evidence for an active fault below the north-western Alpine foreland of Switzerland. *Geophys J Int, 169*, 1273–1288. doi:10.1111/j.1365-264X.2007.03413.x.

Kradolfer U, Mayer-Rosa D (1988) Attenuation of seismic waves in Switzerland. In: *Recent Seismological Investigations in Europe*. Proceedings of the XIX General Assembly of the ESC. Moscow, October 1–6, 1984, pp. 481–488.

Lomax, A., Virieux, J., Volant, P., & Thierry-Berge, C. (2000). Probabilistic earthquake location in 3D and layered models. In C. H. Thurber & N. Rabinowitz (Eds.), *Advances in seismic event location* (pp. 101–134). London: Kluwer Academic Publishers.

Marschall I, Deichmann N, Marone F (in press). Earthquake focal mechanisms and stress orientations in the eastern Swiss Alps. *Swiss J Geosci*.

Maurer, H., Burkhard, M., Deichmann, N., & Green, A. G. (1997). Active tectonism in the western swiss alps. *Terra Nova, 9*, 91–94.

Pavoni, N. (1977). Erdbeben im Gebiet der Schweiz. *Eclogae Geologicae Helvetiae, 70*(2), 351–370.

Pavoni, N., & Roth, P. (1990). Seismicity and seismotectonics of the Swiss Alps. Results of microearthquake investigations 1983–1988. In F. Roure, P. Heitzmann, R. Polino, et al. (Eds.), *Deep Structure of the Alps, Mémoire de la Societé geologique de France, Paris* (pp. 129–134).

Pavoni N, Maurer H, Roth P, Deichmann N (1997) Seismicity and seismotectonics of the Swiss Alps. In: *Deep structure of the Swiss Alps, results of NRP 20, Birkhäuser, Basel*, pp. 241–250.

Poggi, V., Edwards, B., & Fäh, D. (2011). Derivation of a reference shear-wave velocity model from empirical site amplification. *Bull Seismol Soc Am, 101*, 258–274.

Rüttener E (1995). *Earthquake hazard estimation for Switzerland. Matérials Géologie Suisse*, Geophysique, Nr. 29, Schweizerische Geophysikalische Kommission, ETH-Zürich, p. 106.

Rüttener, E., Eogozcue, J., Mayer-Rosa, D., & Mueller, S. (1996). Bayesian estimation of seismic hazard for two sites in Switzerland. *Nat Hazards, 14*, 165–178.

Sägesser, R., & Mayer-Rosa, D. (1978). Erdbebengefährdung in der Schweiz. *Schweizerische Bauzeitung, 78*(7), 3–18.

Waldhauser, F., Kissling, E., Ansorge, J., & Mueller, S. T. (1998). Three-dimensional interface modeling with two-dimensional seismic data: the alpine Crust-Mantle boundary. *Geophys J Int, 135*, 264–278.

Wiemer, S., Giardini, D., Fäh, D., Deichmann, N., & Sellami, S. (2009). Probabilistic seismic hazard assessment of Switzerland: best estimates and uncertainties. *J Seismol, 13*, 449–478. doi:10.1007/s10950-008-9138-7.